# Platelet-Derived Growth Factor C Is Upregulated in Human Uterine Fibroids and Regulates Uterine Smooth Muscle Cell Growth 1

Authors: Suo, Guangli, Jiang, Yong, Cowan, Bryan, and Wang, Jean Y.J.

# Platelet-Derived Growth Factor C Is Upregulated in Human Uterine Fibroids and Regulates Uterine Smooth Muscle Cell Growth[1]

## Guangli Suo,[3] Yong Jiang,[3] Bryan Cowan,[4] and Jean Y.J. Wang[2,3]

*Department of Medicine,[3] Moores Cancer Center, University of California, San Diego, La Jolla, California*
*Department of Obstetrics and Gynecology,[4] University of Mississippi Medical Center, Jackson, Mississippi*

## ABSTRACT

Leiomyomata uteri (i.e., uterine fibroids) are benign tumors arising from the abnormal growth of uterine smooth muscle cells (SMCs). We show here that the expression of platelet-derived growth factor C (*PDGFC*) is higher in approximately 80% of uterine fibroids than in adjacent myometrial tissues examined. Increased expression of *PDGFC* is also observed in fibroid-derived SMCs (fSMCs) relative to myometrial-derived SMCs (mSMCs). Recombinant bioactive PDGFCC homodimer stimulates the growth of fSMCs and mSMCs in ex vivo cultures and prolongs the survival of fSMCs in Matrigel plugs implemented subcutaneously in immunocompromised mice. The knockdown of PDGF receptor-alpha (PDGFRA) through lentiviral-mediated RNA interference reduces the growth of fSMCs and mSMCs in ex vivo cultures and in Matrigel implants. Furthermore, two small molecule inhibitors of the PDGFR tyrosine kinase (i.e., imatinib and dasatinib) exerted negative effects on fSMC and mSMC growth in ex vivo cultures, albeit at concentrations that cannot be achieved in vivo. These results suggest that the PDGFCC/PDGFRA signaling module plays an important role in fSMC and mSMC growth, and that the upregulation of PDGFC expression may contribute to the clonal expansion of fSMCs in the development of uterine fibroids.

*dasatinib, imatinib, lentivirus, PDGF receptor, shRNAmir*

## INTRODUCTION

Uterine fibroids are the most common benign tumors among women of reproductive age. The cumulative incidence of fibroids by age 50 yr is more than 80% for black women and nearly 70% for white women [1]. Although uterine fibroids rarely progress to malignancy, they can cause a variety of symptoms that require clinical intervention. In fact, uterine fibroids are the primary indication for hysterectomy, accounting for more than 200 000 hysterectomies annually in the United States [2]. Fibroids are clonal tumors, each derived from the growth of a single uterine smooth muscle cell (USMC) [3]. Clinical observations suggest that the fibrotic transformation and clonal expansion of fibroid SMCs (fSMCs) is a common event in otherwise healthy women; however, the

mechanisms underlying this transformation and the subsequent clonal expansion are poorly understood [4].

The clonal expansion of fSMCs is likely to be driven by mitogenic pathways downstream of receptor tyrosine kinases (RTKs), because RTK-dependent signaling is a common mechanism in the stimulation of cell proliferation [5]. Therefore, inhibition of RTKs that play a critical role in the proliferation of USMCs may interfere with the growth of fibroid tumors. To identify RTKs that are involved in fibroid growth, we constructed a custom microarray to question the expression of RTKs and their ligands in fibroid and surrounding myometrial tissues collected from 42 patients undergoing hysterectomy for symptomatic fibroids. This focused expression profiling study has led to the molecular classification of patient samples into three groups according to the tissue RNA levels of two genes, *CYR61* and *EFNA4*, which encode extracellular ligands that regulate RTKs and non-receptor tyrosine kinases. The three subgroups defined by our study are: 1) comparable levels of *CYR61* and *EFNA4* RNA in fibroids and adjacent myometrial tissues; 2) *CYR61* RNA downregulated and *EFNA4* RNA upregulated in fibroids; and 3) *CYR61* RNA downregulated but *EFNA4* RNA not upregulated in fibroids. This result suggests that the ligand regulators of protein tyrosine kinase (TK) activities, rather than the expression of protein TKs per se, are misexpressed in fibroid tissues. In addition to *CYR61* and *EFNA4*, we found that the *PDGFC* gene expression is also upregulated in fibroid tissues across the three groups of patient samples.

Platelet-derived growth factors (PDGFs) play crucial roles in the regulation of a wide range of biological processes, including cell proliferation, survival, migration, angiogenesis, tissue remodeling, and organogenesis (e.g., the development of axial skeleton, palate, teeth, and the cardiovascular system) [6, 7]. The *PDGF* gene family consists of four members: *PDGFA*, *PDGFB*, *PDGFC*, and *PDGFD*, which exert their biological functions by binding to and activating two receptor TKs (PDGF receptor alpha [PDGFRA] and PDGFRB). PDGFC contains an N-terminal CUB domain, a hinge region, and a C-terminal growth factor domain, which has to be released by proteolysis to bind to PDGFRA [8, 9]. The proteolytically processed homodimer (PDGFCC) binds to PDGFRA/A homodimers with high affinity but fails to interact with the PDGFRB/B homodimers [8]. Among normal human tissues, *PDGFC* RNA is highly expressed in the heart, the pancreas, the liver, and the kidney [9], and it has been linked to fibrosis and turmorigenesis in various organs [10–12].

In this study, we examined the expression of the four members of the *PDGF* family (*PDGFA*, *PDGFB*, *PDGFC*, and *PDGFD*) and their TK receptors (*PDGFRA* and *PDGFRB*) in fibroid and adjacent myometrial tissues. We also established a panel of primary SMC cultures from the fibroid and myometrial tissues of 31 patients and determined their growth response to PDGFCC in cultures and in Matrigel plugs grown subcutaneously in immunocompromised mice. The results of

this study establish PDGFCC as a mitogen for USMCs, thus suggesting that the upregulation of PDGFC expression in fibroid tissues may promote the clonal expansion of transformed USMCs in the formation of fibroids.

## MATERIALS AND METHODS

### Materials

CodeLink slides were purchased from Amersham. Dulbecco modified Eagle medium (DMEM) and penicillin-streptomycin (PS) were purchased from Cellgro (Mediatech Inc.). Collagenase II, fetal bovine serum (FBS), puromycin, polybrene, and protease cocktail were purchased from Sigma. MicroRNA-adapted short hairpin RNA (shRNAmir) target sets designed for *PDGFRA* and pGIPZ lentiviral vector were purchased from Open Biosystems (Thermo Scientific). Transfection reagent (GeneTran) and plasmid maxi kit were purchased from Biomiga (San Diego, CA). Bicinchoninic acid protein assay kit was purchased from Pierce, and Agilent Low Input cRNA Amplification Kit was purchased from Agilent. The RNAeasy Mini Kit and RNase-Free DNase Set were purchased from Qiagen. SuperScript II kit and PAGE gel were purchased from Invitrogen, and SYBR Green PCR Master Mix was purchased from Applied Biosystems. Anti-PDGFRA (c-20) antibody and goat anti-rabbit horseradish peroxidase (HRP)-conjugated secondary antibody were purchased from Santa Cruz Biotechnology (Santa Cruz, CA). Anti-GAPDH was purchased from Chemicon International. Anti-ACTA2 antibody was purchased from Abcam. Alexa Fluor 448 donkey anti-rabbit immunoglobulin G (IgG), 594 donkey anti-goat IgG, and 594 donkey anti-mouse IgG were purchased from Invitrogen. DAKO universal LSAB kit (DAKO k0679) was purchased from DAKO. Cell Counting Kit 8 (CCK-8) was purchased from Dojindo (Kumamoto, Japan). Bioactive recombinant human PDGFCC protein was purchased from R&D Systems. RAG2$^{-/-}\gamma_c^{-/-}$ (double knockout of *Rag2* and *Il2rg*; the two alleles are *Rag2$^{tm1Fwa}$* and *Il2rg$^{tm1Krf}$*) female mice [13] 6–9 wk old were kind gifts from Dr. Catriona Jamieson at the Moores Cancer Center (University of California, San Diego [UCSD], La Jolla, CA). Matrigel was purchased from BD Biosciences, and D-luciferin was purchased from Caliper LifeSciences. 17β-Estradiol pellets (60-day release; 1.7 mg) were purchased from Innovative Research of America.

### Methods

*Sample collection.* The fibroid and adjacent myometrial tissues were collected from 76 patients (mean age, 42.9 yr; range, 35–52 yr) undergoing hysterectomy. The University of Mississippi Institute Regulation Board approved the sample collections with patient consent. Tissues were explanted from the fibroids and the adjacent myometrium randomly and without any preference. The samples were either frozen in liquid nitrogen for RNA retrieval and/or immersed in DMEM for cell retrieval. Of the 76 sets of samples, 42 sets of RNA were analyzed by the custom microarrays, 76 sets of RNA were analyzed by quantitative real-time RT-PCR (qRT-PCR) reactions, and 31 sets of tissues were converted into primary SMC cultures.

*Custom oligonucleotide array hybridization.* The custom microarrays were constructed by covalent binding of selected 60-mer oligonucleotides to the activated CodeLink slides. Total RNA was extracted from fibroid and adjacent myometrial tissues and was converted into cRNA labeled with either cy5 or cy3 with the Agilent Low Input cRNA Amplification Kit following the manufacturer's instructions. After hybridization, the slides were scanned with an Axon Instruments GenePix 4000B scanner, and the signals were quantified and extracted with the GenePix Pro 5.0 software (Axon Instruments). The fluorescence signals were normalized with the quantile normalization algorithm (R-package DNAMR. J. Cabrera, Rutgers University, http://www.rci.rutgers.edu/~cabrera/DNAMR/) and fitted with a linear mixture-effect model (provided by R-package NLME. Jose Pinheiro, Douglas Bates, Saikat DebRoy, Deepayan Sarkar, and the R Core team 2008. NLME: Linear and Nonlinear Mixed Effects Models. R-package version 3.1-90). The ratios of normalized signals were derived from pairs of fibroid vs. myometrium, hierarchically clustered and displayed with the Genesis program [14].

*Primary culture of USMCs.* Fibroid and myometrial tissues (wet weight, 1 g) were minced into 1-mm$^3$ pieces, placed in 2 ml of PBS containing 0.4% collagenase II, and then incubated at 37°C for 3–5 h. The digested tissue mixtures were washed with 10 ml of DMEM containing 10% (vol/vol) FBS and 1× PS, and the supernatant was discarded after 5 min of centrifugation at 1000 × *g*. The pellets were resuspended in 10 ml of DMEM (containing 10% FBS and 1× PS) and plated in 10-cm plates. The digested tissues were cultured in a humidified 5% CO$_2$ incubator at 37°C without any disturbance until they became attached the bottom of the plate. Fresh media were given every 3 days, and a monolayer of SMCs was established after 1 wk. Confluent monolayers

were dissociated with trypsin and split into fresh dishes. On average, the plates were split once every week. The SMCs were characterized by immunofluorescence staining with anti-ACTA2 antibody. The primary cultures of USMCs were used for qRT-PCR, lentiviral transduction, and proliferation assays between passages two and five.

*Lentivirus-mediated RNA interference targeting PDGFRA.* Five shRNAmir target sets designed for *PDGFRA* were inserted in the pGIPZ lentiviral vector, in which the TurboGFP and the puromycin resistance gene plus shRNAmir are expressed in a single transcript, allowing for the green fluorescent protein (GFP) marking and the puromycin selection of shRNAmir-expressing cells. The plasmids were prepared with plasmid maxi kit and transfected in HEK293FT cells (Invitrogen) with the transfection reagent (GeneTran) to produce lentiviral particles. Briefly, HEK293FT cells were cultured in DMEM medium supplemented with 10% FBS and 1× PS. Cultures with 80% confluent cells in 15-cm dishes were cotransfected with the lentiviral plasmid (20 μg; shRNAmir plasmid or pGIPZ vector plasmid), the lentiviral packaging plasmids pRSV-Rev (5 μg) and pMDLg/pRRE (10 μg), and the vesicular stomatitis virus G glycoprotein expression vector pMD2G (6 μg). The transfection method was performed according to the manufacturer's instructions (Biomiga). The culture supernatants were collected at 2 days after transfection and filtered through a 0.45-μm filter (Millipore). The filtrate was concentrated by centrifugation for 2 h at 25 000 rpm (in an SW-28 rotor; Beckman) and resuspended in PBS. The lentivirus titer determination was performed according to the manufacturer's instructions (Open Biosystems). Briefly, 5000 HEK293 cells were seeded in the 24-well plate and cultured for 1 day. The cells were then infected by serial dilutions of concentrated viral stocks for 1 day. After culturing for 4 days in fresh medium supplemented with puromycin (1 μg/ml), the positive GFP-expressing colonies were counted under fluorescent microscopy. The transducing units per milliliter (TU/ml) was determined by total GFP-positive colonies induced by 1 ml of viral stock. For a typical preparation, the viral titer was from approximately 10$^7$ to 10$^8$ TU/ml. The primary cultures of USMCs at 80% confluency were infected with the concentrated lentiviral stocks at 20–50 multiplicity of infection (MOI) in the presence of 8 μg/ml polybrene for 24 h and then changed to DMEM medium supplemented with puromycin (1 μg/ml) for 6 days to select for cells stably infected with the lentivirus. The infected USMCs were cultured in fresh medium for 5 days after puromycin selection and before qRT-PCR and immunoblotting experiments to determine the efficiency of PDGFRA knockdown.

*RNA extraction and qRT-PCR.* Total RNA from tissues and primary cultures of USMCs were extracted using the RNAeasy Mini Kit according to the manufacturer's instructions. Contaminating genomic DNA was removed on the columns using the RNase-Free DNase Set. Total RNA (2 μg) was reverse transcribed in a 50-μl reaction system using the SuperScript II kit according to the manufacturer's instructions. Polymerase chain reaction (25 μl) containing 2 μl of first-strand cDNA (1:10 dilution), 12.5 μl of SYBR Green PCR Master Mix, and 0.5 μM each of forward and reverse primers was performed for 40 amplification cycles in an ABI PRISM 7700 Sequence Detection System (Applied Biosystems). Cycling conditions were 50°C for 2 min, 49°C for 10 min, 95°C for 15 sec, and 60°C for 1 min. All reactions were run in triplicates. The primers for the PCR amplification of the following genes (*PDGFA*, *PDGFB*, *PDGFC*, *PDGFD*, *PDGFRA*, and *PDGFRB*) were designed using the Primer Express software (version 2.0; please see Supplemental Table S1). The relative expression levels of genes were expressed in arbitrary units, where the C$_t$ value of the gene of interest was normalized to that determined for GAPDH RNA, a housekeeping gene, to correct for differences in concentrations of the cDNA templates.

*Immunohistochemistry.* Frozen sections (5 μm) of myometrial and fibroid tissues were air dried, fixed in 10% formalin for 10 min, and washed in PBS three times each for 5 min. The immunohistochemistry reactions were performed using the DAKO LSAB+ System-HRP kit according to the manufacturer's instructions. Briefly, endogenous peroxidase activity was blocked with 3% hydrogen peroxide for 5 min. After rinsing and aspiration, antibodies diluted in blocking solution (0.05 mol/L Tris-HCl buffer with 1% bovine serum albumin [BSA]) were applied, and the slices were incubated at 4°C for 18 h. Antibodies and dilutions used were PDGFRA (1:150) and PDGFC (1:150). After rinsing with wash buffer (Tris-buffered saline with Tween) and aspiration, the specimens were covered with biotinylated link buffer (biotinylated anti-rabbit immunoglobulin for PDGFRA, and anti-goat immunoglobulin for PDGFC; DAKO) and incubated for 15 min. The sections were rinsed with wash buffer, incubated with streptavidin peroxidase (DAKO) for 15 min, washed, and then reacted with the substrate-chromogen (DAKO) solution for 2 min. The sections were rinsed gently with Tris-buffered saline three times, counterstained with hematoxylin, rinsed with distilled water three times, and then mounted for microscopic evaluation. The sections stained with second antibody only were the control.

*Immunofluorescence.* Cultured SMCs (fSMCs or myometrial SMCs [mSMCs]) were plated onto coverslips and grown at 37°C overnight. Cells were fixed in 4% paraformaldehyde for 10 min, permeabilized in 0.25% Triton X-100/PBS for 5 min, and blocked in 2.5% BSA for 30 min. The coverslips were incubated with the primary antibodies (1:200 dilution of anti-PDGFRA rabbit polyclonal antibody and 1:200 dilution of anti-PDGFC goat polyclonal antibody) in a moist chamber at 4°C for 18 h. The coverslips were washed three times with PBS and then incubated with secondary antibodies (Alexa Fluor 488 donkey anti-rabbit IgG [H+L] at 1:300 dilution and Alexa Fluor 594 donkey anti-goat IgG [H+L] at 1:300 dilution) for 2 h at room temperature in the dark. To examine the expression of ACTA2 in fSMCs or mSMCs, the coverslips were stained with monoclonal ACTA2 antibody (1A4) and subsequently incubated with Alexa Fluor 594 donkey anti-mouse IgG (H+L) at 1:300 dilution. To stain the nuclei, the coverslips were incubated with 0.1 μg/ml Hoechst 33258 for 5 min and rinsed with PBS three times. The coverslips were then mounted, and the fluorescent signals were captured with a CCD camera (Nikon).

*Immunoblotting.* The mSMCs and fSMCs (either uninfected, infected with pGIPZ vector lentivirus, or infected with pGIPZ-shRNA against PDGFRA) were lysed in lysis buffer (20 mM Tris [pH 7.4], 150 mM NaCl, 10% glycerol, 0.5% Nonidet P-40, 1× protease cocktail, 0.55 mM DL-dithiothreitol) and incubated for 20 min on ice. The lysates were cleared by centrifugation at 21 000 × g for 15 min at 4°C, and the supernatants were quantitated using the bicinchoninic acid protein assay kit. Whole-cell lysates (40 μg) were fractionated on 4%–20% gradient SDS-PAGE gels and transferred to nitrocellulose membranes. The membranes were incubated with anti-PDGFRA (c-20) antibody, followed by goat anti-rabbit HRP-conjugated secondary antibody, and were visualized by chemiluminescence. Stripped membranes were reprobed with anti-GAPDH followed by goat anti-mouse IgG-HRP as loading control.

*Cell proliferation.* Cell proliferation was measured by the CCK-8 kit according to the manufacturer's instructions. Briefly, USMCs were seeded in 96-well plates (5000 cells/well) in DMEM containing 10% FCS for 2 h and then washed twice with PBS and incubated for 2 h in serum-free DMEM, followed by incubation in serum-free medium with or without the supplement of recombinant bioactive mature human PDGFCC protein (100 ng/ml) at 37°C, 5% $CO_2$. The CCK assay was performed at time 0 and at 4, 12, 24, 36, and 48 h after the addition (or not) of PDGFCC. The absorbance at 450 nm was converted to the numbers of viable cells according to a standard curve constructed in parallel by seeding different numbers of cells in wells right before the time of CCK assays.

*Growth inhibition by TK inhibitors.* To determine the growth inhibitory effects of TK inhibitors imatinib and dasatinib, USMCs were incubated with varying concentrations of the drugs (0–100 μM for imatinib; 0–10 μM for dasatinib) in 96-well plates (5000 cells/well). Prior to drug addition, cells were cultured for 12 h in DMEM medium with 10% FBS and then shifted to medium with either 10% or 0.5% FBS during drug treatment for a total period of 96 h, with fresh drug-supplemented medium replaced every 24 h. For the majority of USMC cultures, growth rates were reduced in the medium with 0.5% FBS, and the $IC_{50}$ values were not significantly altered by the FBS concentrations. At the end of 96 h, 10 μl of CCK-8 solution was added to each well and cells, and the number of viable cells was determined as described above. The $IC_{50}$ was defined as the concentration of imatinib or dasatinib resulting in a 50% decrease in the level of USMC viability compared with untreated control.

*Matrigel implants in RAG2$^{-/-}$γ$_c^{-/-}$ mice.* RAG2$^{-/-}$γ$_c^{-/-}$ female mice were bred and maintained on sulfamethoxazole water under specific pathogen-free conditions in the animal care facility at UCSD Moores Cancer Center. Female athymic nude mice 6–9 wk old were acquired from the UCSD Animal Care Program. All experiments on mice were conducted in accordance with the guidelines of National Institutes of Health (Bethesda, MD) for the care and use of laboratory animals. The animal study protocol (s02013) was approved by UCSD and the Medical Experimental Animal Care Committee. The 17β-estradiol pellets (60-day release; 1.7 mg) were implanted subcutaneously on the back of the neck areas 3 days prior to the engraftment experiments. The fSMCs were infected with concentrated GFP-Luciferse lentiviral stock [15] at 50 MOI in the presence of 8 μg/ml polybrene for 12 h at 37°C. The infected fSMCs were then cultured in DMEM with 10% FBS for 36 h. To test the effect of PDGFRA knockdown on the fSMC expansion in the Matrigel implants in RAG2$^{-/-}$γ$_c^{-/-}$ female mice, the vector and shRNA- infected fSMCs were cultured in DMEM with 10% FBS for 12 h before transplantation. To test the effect of bioactive recombinant PDGFCC, the fSMCs were cultured in serum-free DMEM for 12 h before transplantation. Subsequently, the infected fSMCs were dissociated with trypsin, collected in PBS, and then mixed with an equal volume (0.5 ml) of Matrigel at 4°C. A total of 5 × 10$^6$ fSMCs in 150 μl of 50% Matrigel with or without the supplement of recombinant bioactive mature human PDGFCC protein (100 ng/ml) were transplanted into RAG2$^{-/-}$γ$_c^{-/-}$ female mice subcutaneously on both flanks. The control mice were transplanted

with 200 μl of PBS-Matrigel. Whole-body bioluminescence signaling was detected using the IVIS 200 Imaging System series (Caliper) at different time points (0, 2, 4, 6, 9, 12, and 15 days), as described previously [16, 17]. Mice were anesthetized with isoflurane and injected intraperitoneally with D-luciferin (150 mg/kg body weight) approximately 10 min before imaging. Each mouse was subjected to four IVIS analyses; exposures of 3 min, 1 min, 20 sec, and 5 sec, every 2 or 3 days after injection of cells. Dorsal images were analyzed by using total photon flux emission (photons/sec) in the region of interest (ROI) by LivingImage Software (Xenogen). The datum in each ROI was normalized by the same ROI datum collected at first day when we injected the fSMCs. Curve diagrams were generated to evaluate the effect of PDGFCC or PDGFRA knockdown on the fSMC expansion in the Matrigel implants in RAG2$^{-/-}$γ$_c^{-/-}$ female mice.

*Statistical analyses.* A two-tailed and paired Student *t*-test was used to analyze statistical differences of relative expression levels of *PDGFA*, *PDGFB*, *PDGFC*, *PDGFRA*, and *PDGFRB* between myometrium and fibroid tissues or SMCs from various numbers of patients, and it was also used to analyze statistical differences of the $IC_{50}$ values for imatinib and dasatinib. A one-tailed and unpaired Student *t*-test was used to analyze statistical differences of proliferation between the SMCs with or without PDGFCC or between PDGFRA knockdown SMCs and the control SMCs. A one-way ANOVA followed by a Tukey comparison test was used to calculate the *P* values. To calculate the imatinib or dasatinib $IC_{50}$ values, the optical density at 450 nm ($OD_{450}$) absorbance results were log-transformed and fitted a curve with nonlinear regression by Sigmoidal dose-response (variable slope) equation. The Pearson correlation test was performed to determine the correlation between the expression levels of *PDGFC* and *PDGFRA*, the $IC_{50}$ values, and the ratios of these values between pairs of fibroid vs. myometrial tissues and primary cell cultures. These various statistical analyses were performed using the GraphPad Prism 4 package (GraphPad Software).

## RESULTS

### Levels of PDGF and PDGFR RNAs in Uterine Tissues

We have examined the expression profiles of 90 human TKs and 103 ligands known to activate TKs in the fibroid and adjacent myometrial tissues from 42 patients. The microarray hybridization results suggested that the *PDGFC* RNA levels were higher in fibroid than in matching myometrial tissues from 28 of the 42 patients surveyed (Fig. 1A). However, the RNA levels of *PDGFA*, *PDGFB*, and *PDGFD*, and those of the *PDGF* receptors (*PDGFRA* and *PDGFRB*) were not significantly altered between the matched fibroid and myometrial tissues (Fig. 1A). To confirm the microarray results, we applied qRT-PCR to measure the RNA levels of *PDGFA*, *PDGFB*, *PDGFC*, *PDGFD*, *PDGFRA*, and *PDGFRB* in 49–76 pairs of fibroid and adjacent myometrial tissues. The mean level of *PDGFC* RNA in the fibroids was significantly higher than that in the myometrial tissues ($P < 0.01$; Fig. 1B). The ratio of *PDGFC* RNA (fibroid:adjacent myometrium) in 57 of 70 pairs was equal to or higher than 1.5-fold. By contrast, the *PDGFB* and *PDGFD* RNA levels in fibroid tissues were lower than those in myometrial tissues, and the levels of the *PDGFA* RNA were similar between matched fibroid and myometrial tissues (Fig. 1B).

Unlike *PDGFC*, the levels of *PDGFR* RNAs were not increased in fibroid tissues. Instead, the *PDGFRB* RNA levels were slightly higher in myometrial tissues ($P < 0.01$) from 58 patients, whereas the *PDGFRA* RNA levels were similar between fibroid and adjacent myometrium tissues from 76 patients (Fig. 1C). Pearson correlation analysis showed that there was no correlation between the levels of *PDGFC* and *PDGFRA* RNAs in fibroid or adjacent myometrial tissues from 69 patients (Fig. 1, D and E). To determine that the *PDGFC* RNA levels reflect the production of PDGFC proteins in the fibroid and myometrial tissues, we performed immunohisto-chemistry analyses of six pairs of myometrial and fibroid tissue sections and found higher levels of anti-PDGFC signals in fibroid than adjacent myometrial tissues in each pair of samples. Representative results from two pairs of tissues are
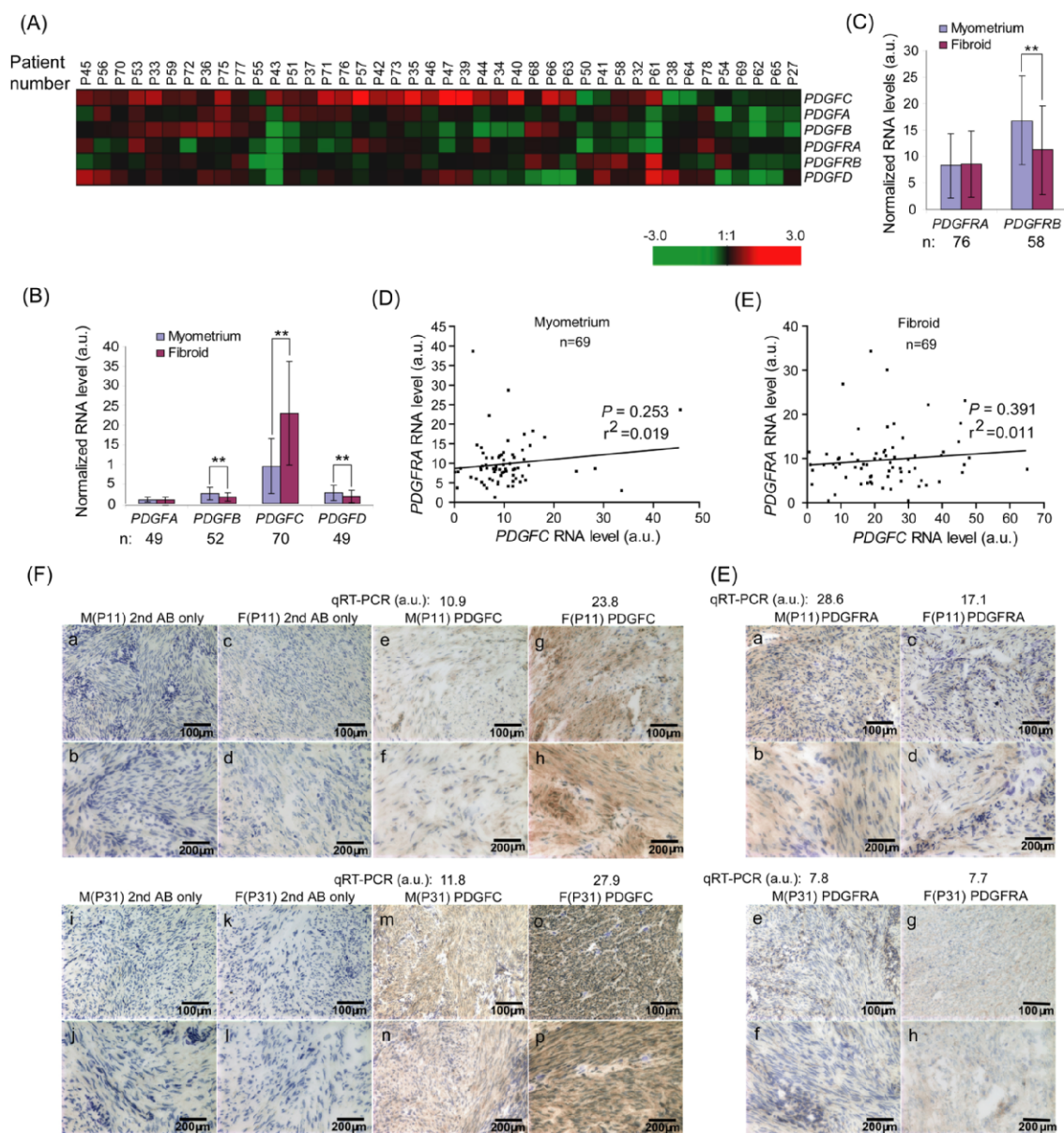
FIG. 1. Increased expression of *PDGFC* in uterine fibroids. **A**) *PDGF* and *PDGFR* expression patterns from 42 pairs of uterine samples determined by microarray analyses. Red color depicts a statistically significant upregulation, whereas green color depicts downregulation, of the indicated genes. **B** and **C**) The RNA levels of the indicated *PDGF* (**B**) and *PDGFR* (**C**), determined by quantitative RT-PCR relative to those of GAPDG, are shown as arbitrary units (a.u.). n, number of tissues examined. **P < 0.01. **D** and **E**) Lack of correlation between the expression of *PDGFC* and its receptor *PDGFRA* in uterine tissues; $r^2$ values are derived from linear regression. **F** and **G**) Immunohistochemistry detection of PDGFC (**F**) and PDGFRA (**G**) in myometrial (M) and fibroid (F) tissues from the indicated patient samples. The levels of *PDGFC* and *PDGFRA* RNA in each sample were shown by data of qRT-PCR (a.u.). The sections stained with the second antibody (2nd AB) only were the controls. Bars = 100 μm (original magnification ×200) for the upper row in each set, or 200 μm (original magnification ×400) for the lower row in each set.

shown in Figure 1F. We also detected the expression of PDGFRA in the tissue sections (Fig. 1G), consistent with a previously published report [18]. These results show that PDGFC expression is upregulated in the majority of fibroid tissues, but there is not a coordinated upregulation of its receptor, PDGFRA, in fibroids.

### PDGFC and PDGFRA Expression in Primary Cultures of USMCs

We prepared pairs of primary cultures of fSMCs and mSMCs from 31 patient samples, and we measured the RNA levels of *PDGFC* and *PDGFRA* by qRT-PCR (Fig. 2, A and

C). We found that the levels of *PDGFC* RNA were 1.7-fold higher in the fSMC group than in the mSMC group ($P < 0.05$; Fig. 2A), whereas the levels of *PDGFRA* RNA were similar between the two groups of cells (Fig. 2C). From the scatter plots, it is clear that the levels of *PDGFC* RNA were much higher in tissues than in the primary cultures (Fig. 2, A and B). Using the Pearson correlation test, we found no correlation between the levels of *PDGFC* RNA among the tissues and the corresponding primary cultures of SMCs (Fig. 2, E and F). The lack of correlation also applied to the RNA levels of *PDGFRA* (Fig. 2, G and H). There was a significant correlation between the levels of *PDGFC* and *PDGFRA* RNAs among the group of mSMCs (Fig. 2I) but not with the group of fSMCs (Fig. 2J). To
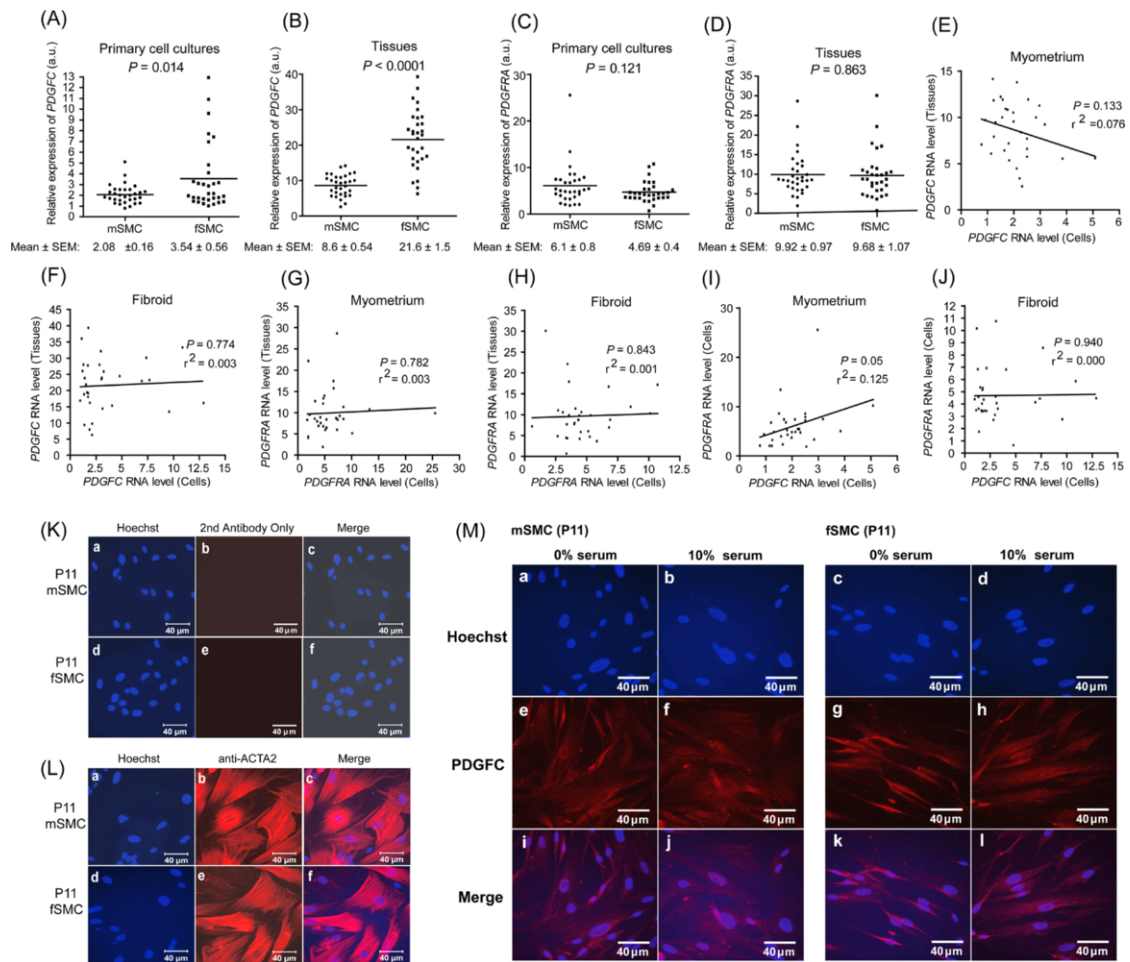
FIG. 2. *PDGFC* expression in primary cultures of mSMCs and fSMCs. **A–D**) Scatter plots of the RNA levels of *PDGFC* and *PDGFRA* as determined by quantitative RT-PCR in the indicated primary cultures or tissues, with the mean and SEM shown from 31 patient samples (n = 31). The *P* values were calculated by two-tailed and paired Student *t*-test. a.u., arbitary units. **E–J**) Correlation between the levels of the indicated RNA in tissues and cell cultures derived from myometrium or fibroid samples. **K–M**) Immunofluorescence detection of DNA (Hoechst), alpha-actin (ACTA2), and PDGFC in a pair of mSMC and fSMC. Bars = 40 μm; original magnification ×400.

examine the expression of PDGFC in the mSMC and fSMC cultures, we performed immunofluorescence analyses. Representative results with one pair of mSMCs and fSMCs are shown in Figure 2, K–M. The mSMCs and fSMCs expressed the alpha-actin (ACTA2) gene, which is a marker of SMCs (Fig. 2L). These cells also expressed the PDGFC protein (Fig. 2M). Because serum contains PDGFs, we performed the anti-PDGFC staining using cells that were incubated in serum-free medium for 24 h prior to fixation and found that the anti-PDGFC reactivity was not diminished under serum-free conditions (Fig. 2M). Fluorescent secondary antibodies alone did not react with the mSMCs and fMSCs (Fig. 2K), demonstrating that the PDGFC and ACTA2 signals were specific to each of the two primary antibodies.

Taken together, results in Figures 1 and 2 show that *PDGFC*, but not *PDGFRA*, is upregulated in the majority of fibroid tissues examined. The increased expression of *PDGFC* in fibroid tissues is likely to be caused by a combination of alterations: some are SMC autonomous, whereas others may be dependent on the tissue environment. As a result, the levels of *PDGFC* RNA detected in the fibroid tissues are not stably maintained in the primary SMC cultures (Fig. 2F), but the *PDGFC* RNA levels remain higher among the fSMC than the mSMC cultures (Fig. 2A).

## Recombinant Bioactive PDGFCC Stimulates USMC Growth

To determine whether PDGFCC stimulates the growth of fSMCs and mSMCs, we examined the effect of recombinant PDGFCC homodimer, composed of its C-terminal growth factor domain, on the proliferation of mSMC and fSMC cultures derived from three patients (Fig. 3, A–F). The control cultures (serum-free medium without PDGFCC) exhibited a low rate of growth during the experimental time course. The addition of PDGFCC stimulated the growth of mSMC and fSMC cultures, with the rate of proliferation significantly increased by the supplement of PDGFCC in each of the three pairs of SMC cultures tested (Fig. 3, A–F).

We also examined the expansion of fSMCs in Matrigel plugs implanted subcutaneously into immunocompromised mice (Fig. 3, G and H). We infected fSMC cultures with lentivirus carrying a GFP-Luciferase fusion gene [15], injected the infected cells with Matrigel subcutaneously into RAG2$^{-/-}$γ$_c$$^{-/-}$ female mice that were previously implemented with estrogen pellets, and followed the expansion of the injected cells by bioluminescence imaging for Luciferase activity (Fig. 3, G and H). In Matrigel plugs without PDGFCC, an initial expansion of Luciferase signal at Day 2 was quickly followed by a decline in bioluminescence signals (Fig. 3H). In Matrigel plugs with the
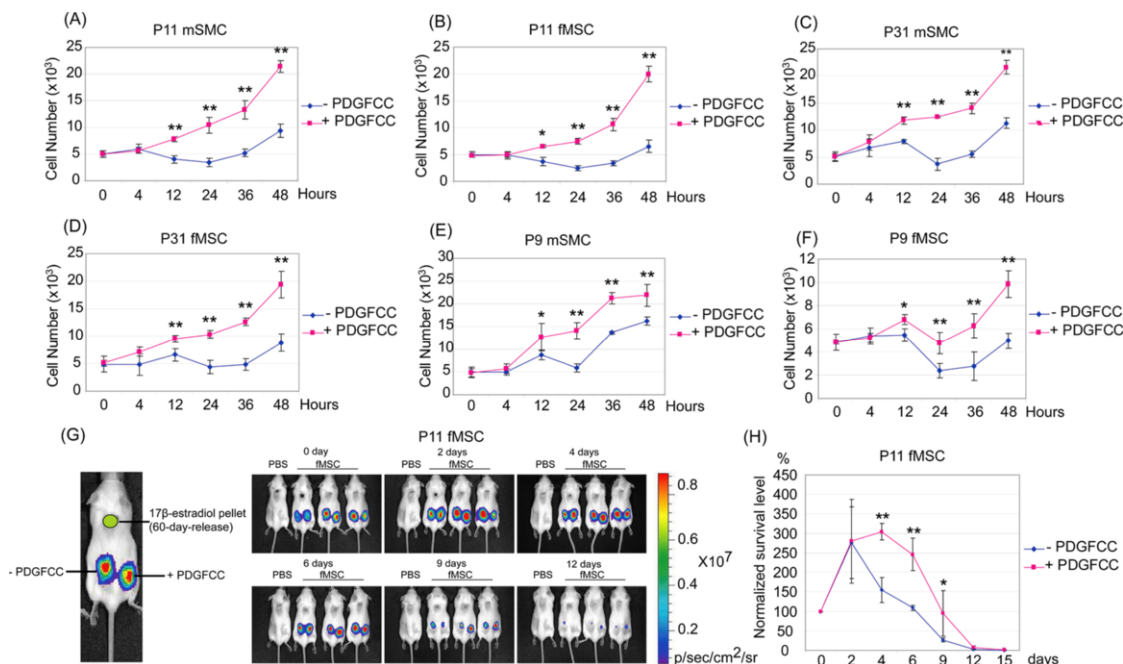
FIG. 3. Recombinant PDGFCC stimulates the proliferation of uterine SMCs. The indicated primary SMC cultures derived from the fibroid and adjacent myometrial tissues were stimulated with (+) or without (−) recombinant, bioactive PDGFCC homodimer. Cell proliferation values shown are the means and SDs from three independent experiments with four wells of cells taken at each of the indicated time points. **A**, **C**, and **E**) Primary culture SMCs derived from three myometrial tissues. **B**, **D**, and **F**) Primary SMC cultures derived from the corresponding fibroid tissues. The indicated primary cell cultures infected with GFP-luciferase lentivirus were mixed with Matrigel with (+) or without (−) recombinant bioactive PDGFCC and were then transplanted subcutaneously into RAG2$^{-/-}$γ$_c$$^{-/-}$ female mice. **G**) Representative imaging pictures of luciferase activity in the transplanted Matrigel plugs. **H**) Quantitation of bioluminescence signals. The values shown are mean and SDs from three mice per experiment. *$P < 0.05$; **$P < 0.01$. p/sec/cm$^2$/sr, number of photons per second per square centimeter of steradian.

supplement of PDGFCC, the initial expansion of Luciferase signals was not significantly enhanced; however, the decay of the signals was significantly slower during the next 7 days (n = 3; $P < 0.05$; Fig. 3H). These results show that PDGFCC promotes the survival of fSMCs as Matrigel implants in immunocompromised mice.

### Effect of PDGFRA Knockdown on the Proliferation of USMCs

Given the knowledge that PDGFC binds PDGFRA and does not interact with PDGFRB homodimers [9], we examined the role of PDGFRA in the proliferation of fSMCs and mSMCs. We employed lentivirus-mediated RNA interference to knock down PDGFRA expression in two pairs of mSMC and fSMC cultures derived from two patient samples (P11 and P31; Fig. 4). By testing five different microRNA-adapted shRNAmir target sets designed for PDGFRA in the human glioblastoma cell line U118, we identified one target set (Open Biosystems clone ID V2LHS_58978, with the shRNA sequence TGCTGTTGACAGTGAGCGACCTCTATCCTTCCAAAT-GAAATAGTGAAGCCACAGATGTATTTCATTTGGAAG-GATAGAGGGTGCCTACTGCCTCGGA) that could decrease *PDGFRA* RNA level by approximately 75% (data not shown). We then used this shRNAmir to knock down PDGFRA in mSMCs and fSMCs. As shown in Figure 4, A–C, cells infected with lentivirus carrying the shRNAmir cassette contained lower levels of the *PDGFRA* RNA (Fig. 4A) and the PDGFRA protein (Fig. 4B) than the uninfected controls or cells infected with lentivirus derived from the pGIPZ vector. The *PDGFRA* RNA was reduced by 74% in P11 mSMCs, 72% in P11 fSMCs, 48% in P31 mSMCs, and 52% in P31 fSMCs

compared with uninfected or vector-infected controls (Fig. 4A), corresponding to lower levels of PDGFRA protein (Fig. 4B).

The reduction in PDGFRA protein expression was also observed by immunofluorescence staining with anti-PDGFRA of control and knocked-down cells (Fig. 4C).

We then examined the proliferation of these SMCs in cultures and found that the knockdown of PDGFRA consistently reduced the rate of proliferation in the mSMC and fSMC cultures from the two patients tested (Fig. 4, D–G). We also examined the expansion of control and PDGFRA-knocked down fSMCs in Matrigel plugs implanted in the RAG2$^{-/-}$γ$_c$$^{-/-}$ female mice (Fig. 4, H and I). We observed the expansion of control and PDGFRA-knocked down fSMCs in the implanted Matrigel plugs during a period of 6 days (Fig. 4, H and I). However, the extent of the increase in Luciferase signals was significantly lower with PDGFRA-knocked down cells (n = 3; $P < 0.05$; Fig. 4I).

### Effects of TK Inhibitors on USMC Proliferation

A number of small molecular inhibitors for protein TKs have been used successfully in the clinical setting to treat cancers. Among them, imatinib and dasatinib can inhibit the activity of PDGFRA TK [19–21]. We therefore tested the effects of imatinib and dasatinib on the proliferation of mSMCs and fSMCs. We treated 27 pairs of mSMC and fSMC cultures with varying concentrations of the drugs for a period of 96 h and employed a nonlinear regression model to calculate the IC$_{50}$ value for each drug. The dose-response curves for imatinib and dasatinib on one pair of mSMC and fSMC cultures are shown in Figure 5, A, B, D, and E. As described previously, the proliferation of primary foreskin fibroblasts is not inhibited by clinically relevant doses of imatinib or
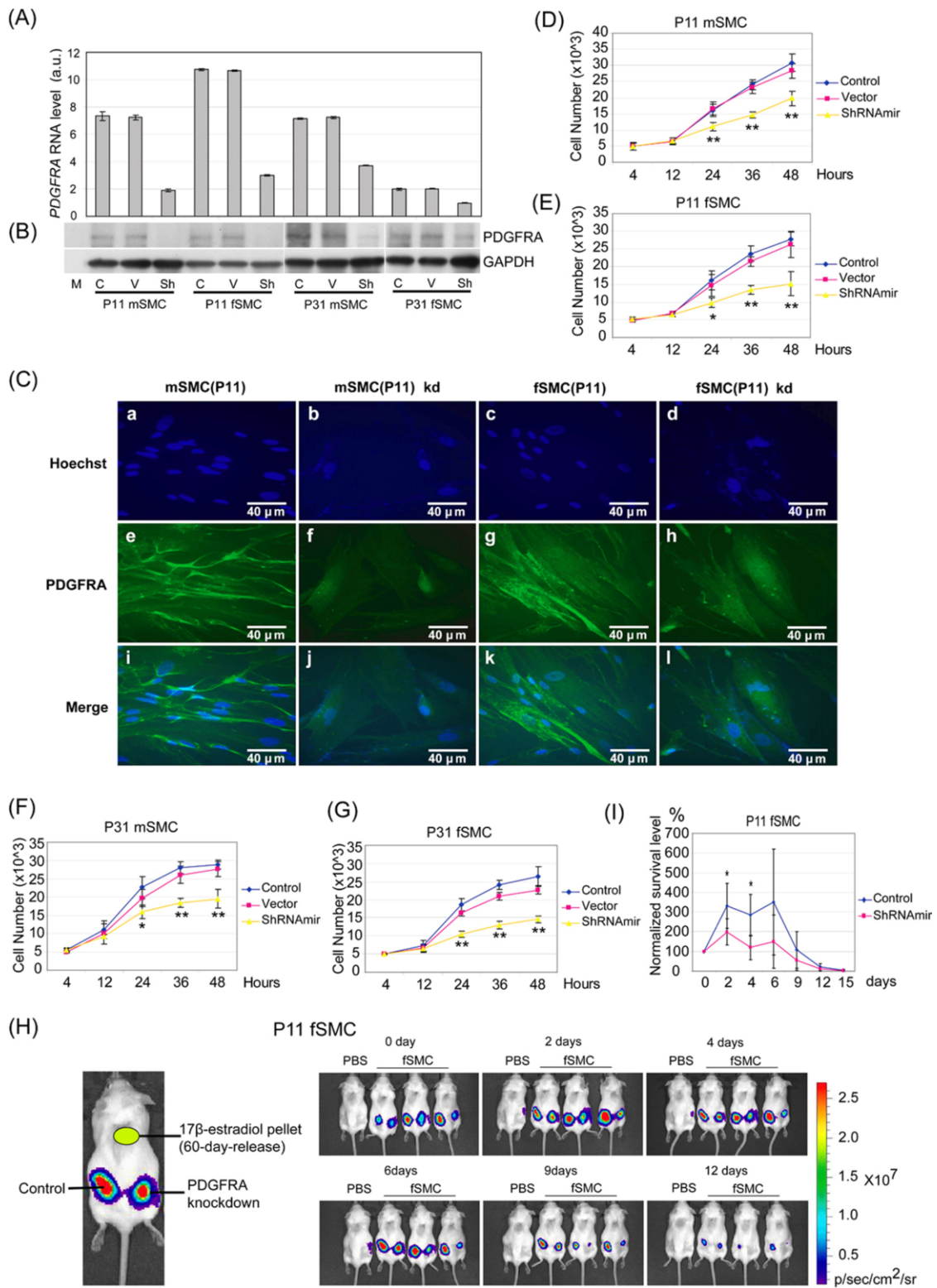
FIG. 4. Knockdown of PDGFRA reduced uterine SMC proliferation. The indicated primary cell cultures derived from two pairs of patient samples were uninfected (control [C]) or were infected with vector-lentivirus (V) or PDGFRA-shRNA-lentivirus (Sh). **A**) The levels of *PDGFRA* RNA determined by quantitative RT-PCR. Results shown are means and SDs from three independent measurements. a.u., arbitrary unit. **B**) Immunoblots of whole cell lysates from the indicated cell populations probed with antibodies against PDGFRA (upper) or GAPDH (lower) as a loading control. **C**) Immunofluorescence detection of PDGFA in control and knocked down (kd) cells. Bars = 40 μm; original magnification ×400. **D–G**) Cell proliferation of uninfected (control), vector-lentivirus-infected (vector), and PDGFRA-shRNA-lentivirus-infected (shRNAmir) cell populations derived from the indicated patient sample was determined. The values shown are means and SDs from three independent experiments with four wells of cells assayed per time point. The indicated primary cell cultures infected with GFP-luciferase lentivirus were mixed with Matrigel and then transplanted subcutaneously into RAG2$^{-/-}$γ$_c$$^{-/-}$ female mice. **H**) Representative imaging pictures of bioluminescence signals in Matrigel plugs. **I**) Quantification of bioluminescence signals. The values shown are means and SDs from three mice per experiment. *$P < 0.05$; **$P < 0.01$. In **D–G**, 10^3 is $10^3$.
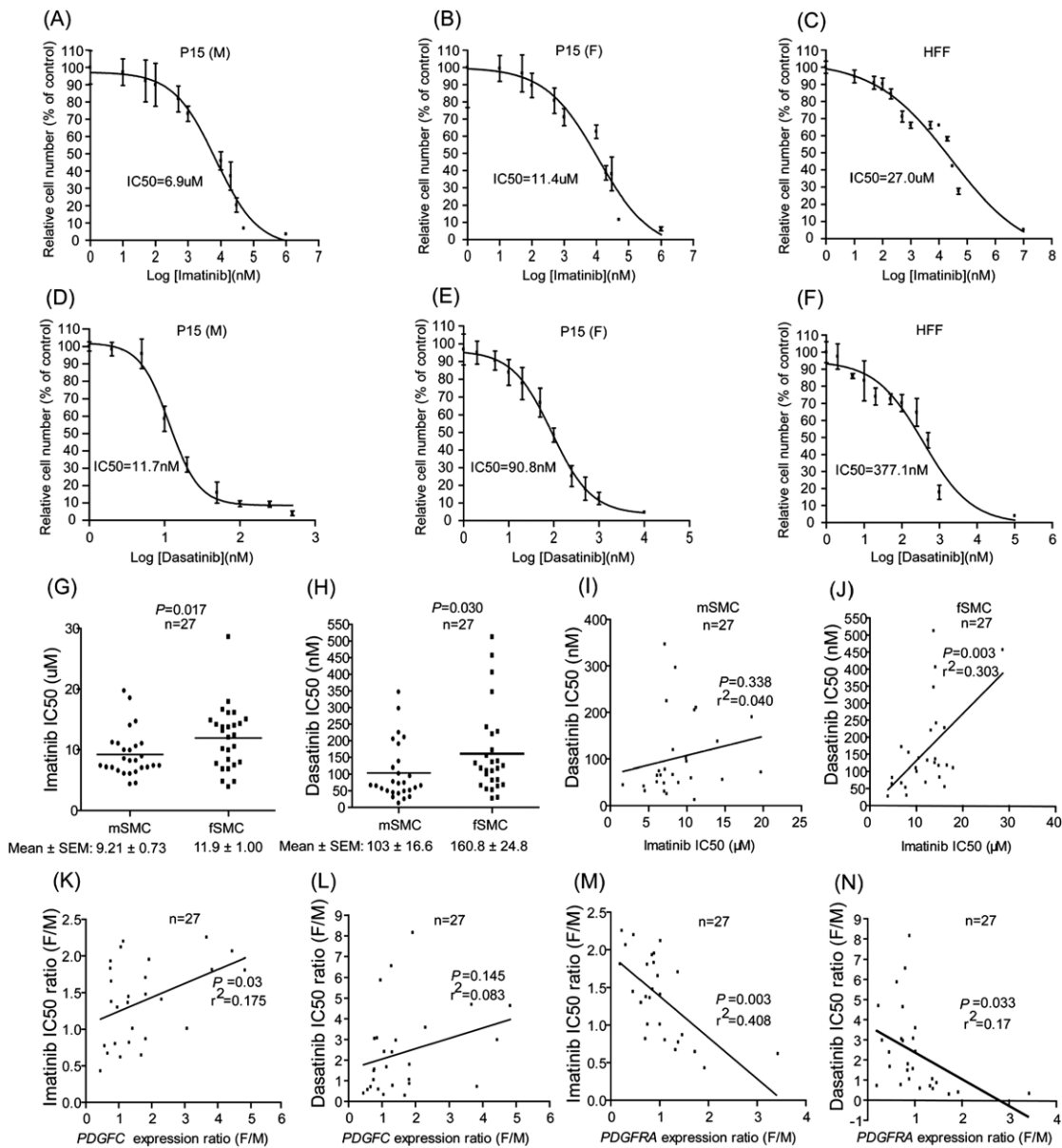
FIG. 5.    Tyrosine kinase inhibitors imatinib and dasatinib interfere with proliferation of uterine SMCs. **A–C**) Imatinib dose-response curves from representative cultures of mSMC, (**A**) fSMC (**B**), and primary human foreskin fibroblasts (HFF; **C**). The values shown are means and SDs from three independent experiments with four wells of data collected for each drug concentration in each experiment. **D–F**) Dasatinib dose-response curves as in **A–C**. **G** and **H**) Scatter plots of imatinib (**G**) or dasatinib (**H**) $IC_{50}$ values determined among 27 pairs of primary mSMC/fSMC cultures. **I** and **J**) Correlation between drug responses among the primary cultures derived from myometrial tissues (**I**) or fibroid tissues (**J**). **K** and **L**) Correlation between the ratios (fibroid:myometrium; F/M) of $IC_{50}$ and *PDGFC* RNA levels among pairs of primary smooth muscle cultures derived from 27 patient samples. **K**) Imatinib. **L**) Dasatinib. **M** and **N**) Correlation between the ratios (fibroid:myometrium) of $IC_{50}$ and *PDGFRA* RNA levels as in **K** and **L**. **M**) Imatinib. **N**) Dasatinib. $P < 0.05$ means that the correlation is statistically significant. In **A–C** and **G**, uM is µM.

dasatinib. In our experiments, the $IC_{50}$ of growth inhibition in human foreskin fibroblasts by imatinib was 27 µM, and that for dasatinib was 377 nM (Fig. 5, C and F). Under ex vivo culture conditions, we determined that the $IC_{50}$ for imatinib was around 10 µM for the inhibition of mSMC and fSMC proliferation (Fig. 5G), and that for dasatinib was between 100 and 160 nM (Fig. 5H) among the 27 pairs of primary cultures tested. These $IC_{50}$ values are also much higher than the clinically relevant dose. Consistent with these high $IC_{50}$ values, we found that administration of imatinib or dasatinib to mice did not interfere with the transient increase in Luciferase signals in Matrigel plugs implanted in those mice (data not shown). Nevertheless, the ex vivo results show that mSMCs

and fSMCs are more sensitive to these TK inhibitors than foreskin fibroblasts.

With the mSMC cultures, Pearson correlation test shows that the sensitivity to imatinib and dasatinib was not concordant among the 27 primary cultures of mSMCs (Fig. 5I). However, among the cultures of fSMCs, there was a significant correlation between the responses to imatinib and dasatinib (Fig. 5J). We also compared the ratio of *PDGFC* RNA levels to that of the drug $IC_{50}$ values among the 27 pairs of fSMCs vs. corresponding mSMC cultures and found a positive correlation, indicating that fSMCs that contained higher levels of *PDGFC* RNA were more resistant to the TK inhibitors (Fig. 5, K and L). In contrast, there was a negative correlation between the ratio of *PDGFRA* RNA levels and the $IC_{50}$ values,

indicating that fSMCs that contained higher levels of *PDGFRA* RNA were more sensitive to the TK inhibitors.

## DISCUSSION

Through a focused comparison of the expression profiles of protein TKs and their ligand activators, followed by quantitative real-time PCR and immunohistochemistry analyses of a large number of fibroid and myometrial tissues, we have shown that the levels of *PDGFC* RNA and protein are consistently upregulated in the majority of fibroid rather than adjacent myometrial tissues. This conclusion is in agreement with a previous report, where 16 pairs of fibroid and myometrial tissues were examined, and the upregulation of *PDGFC* RNA was observed in fibroid tissues [22]. Thus, the upregulation of PDGFC is a hallmark of uterine fibroids.

We have also shown that the levels of *PDGFC* RNA are higher in fibroid-derived primary SMC cultures than those derived from myometrial tissues. Interestingly, we found that the levels of *PDGFC* RNA in tissues were not maintained in the primary SMC cultures, suggesting that the tissue microenvironment and/or other cell types also play important roles in PDGFC expression in the fibroid tissues. Consistent with our finding, a microarray-based gene profiling study has found that ex vivo propagation of mSMCs and fSMCs causes large changes in gene expression and reduces the differences observed in the original myometrium and fibroid tissues [23]. Thus, the ex vivo cultures of USMCs are useful in studying cell-autonomous mechanisms, but they are not suitable for elucidating alterations that are dependent on inputs from the tissue microenvironment.

Using primary SMC cultures, we have demonstrated that bioactive recombinant PDGFCC stimulates the proliferation of mSMCs and fSMCs. Furthermore, reduction of the PDGFRA through lentiviral-mediated RNA interference decreases the proliferation of mSMCs and fSMCs. The expression of PDGFRA in USMCs has been established previously by immunohistochemistry studies [18] and was confirmed in this study. Our results suggest that PDGFRA, which is expressed in both the mSMCs and the fSMCs in the tissues and in ex vivo cultures, is likely to play an important role in uterine smooth muscle proliferation. The contribution of PDGFRB to vascular SMC proliferation is well established [24]. By analogy, PDGFRA may stimulate the proliferation of USMCs; for example, during blood clotting and the release of PDGFs from the aggregated platelets. Furthermore, our results suggest that the activated PDGFRA may also stimulate the clonal expansion of fSMCs. In this regard, the upregulation of PDGFC expression in fibroid tissues may contribute to an autocrine mitogenic pathway to drive the development of fibroids.

It is important to note that PDGFC is translated as a multidomain protein that does not bind to PDGFRA with high affinity [9]. The latent PDGFC has to be processed by proteases (e.g., tissue plasminogen activator [tPA] or plasmin) to become activated for binding to PDGFRA [9, 25–27]. We have detected the full-length PDGFC protein as well as varying levels of lower-molecular weight forms of PDGFC in fibroid tissue extracts by Western blotting (data not shown). However, we do not know whether the lower-molecular weight forms of PDGFC were specifically released from an activating protease or are nonspecific degradative products generated during tissue collection. We have detected higher levels of PDGFC protein in the fibroid than in adjacent myometrial tissues. Because the active PDGF/PDGFR complex is endocytosed and degraded in the lysosome, the PDGFC protein detected in the fibroid tissues is likely to be the latent form. The accumulation of latent PDGFC in fibroid tissues may provide a reservoir of a potent growth and survival factor that can be quickly activated by proteases, such as tPA and plasmin, to stimulate fibroid growth under thrombolytic conditions. Alternatively, the abnormal expression of other proteases that can cleave and activate the latent PDGFC may deregulate proliferation of fSMCs. It would therefore be of interest to search for PDGFC-processing enzymes in fibroids as a future direction to further delineate the role of PDGFC in the development of uterine fibroids.

The PDGF-PDGFR signaling module plays important roles in a number of pathogenic conditions, including atherosclerosis, fibrosis, and cancer [6]. Consequently, a number of pharmacological inhibitors of the PDGF-PDGFR signaling module have been developed, including 1) neutralizing antibodies against PDGFs, 2) soluble decoy receptors, 3) antibodies against PDGFR, and 4) small molecular inhibitors of the PDGFR TK [6]. In this study, we examined two TK inhibitors, imatinib and dasatinib, known to inhibit PDGFR and several other TKs [21, 28], for their effects on the proliferation of USMCs. We have found that USMCs are more sensitive to these two TK inhibitors than primary human foreskin fibroblasts. However, the $IC_{50}$ values for the inhibition of USMC proliferation by both TK inhibitors are above the clinically relevant concentrations. Nevertheless, we did observe a significant correlation between the levels of *PDGFRA* expression with drug sensitivities among the 54 primary SMC cultures tested, supporting the idea that the TK inhibitors target the PDGFRA TK to inhibit USMC proliferation. The two TK inhibitors tested here are not specific for the PDGFRA TK; in fact, they inhibit several other receptor and nonreceptor TKs [21]. Recently, imatinib also has been shown to inhibit a nonkinase target (i.e., NQO2) [29]. The promiscuity of these TK inhibitors might have contributed to the wide range of $IC_{50}$ values observed with this large panel of primary SMCs. Although the two TK inhibitors tested may not be effective in blocking the growth of fSMCs, our results suggest that PDGFC and PDGFRA are potential targets for the development of medical therapies to treat uterine fibroids.

## ACKNOWLEDGMENTS

## REFERENCES

1. Day Baird D, Dunson DB, Hill MC, Cousins D, Schectman JM. High cumulative incidence of uterine leiomyoma in black and white women: ultrasound evidence. Am J Obstet Gynecol 2003; 188:100–107.
2. Walker CL, Stewart EA. Uterine fibroids: the elephant in the room. Science 2005; 308:1589–1592.
3. Linder D, Gartler SM. Glucose-6-phosphate dehydrogenase mosaicism: utilization as a cell marker in the study of leiomyomas. Science 1965; 150:67–69.
4. Canevari RA, Pontes A, Rosa FE, Rainho CA, Rogatto SR. Independent clonal origin of multiple uterine leiomyomas that was determined by X chromosome inactivation and microsatellite analysis. Am J Obstet Gynecol 2005; 193:1395–1403.
5. Blume-Jensen P, Hunter T. Oncogenic kinase signalling. Nature 2001; 411:355–365.
6. Andrae J, Gallini R, Betsholtz C. Role of platelet-derived growth factors in physiology and medicine. Genes Dev 2008; 22:1276–1312.
7. Hoch RV, Soriano P. Roles of PDGF in animal development. Development 2003; 130:4769–4784.
8. Gilbertson DG, Duff ME, West JW, Kelly JD, Sheppard PO, Hofstrand PD, Gao Z, Shoemaker K, Bukowski TR, Moore M, Feldhaus AL, Humes JM, et al. Platelet-derived growth factor C (PDGF-C), a novel growth

factor that binds to PDGF alpha and beta receptor. J Biol Chem 2001; 276: 27406–27414.

9. Li X, Ponten A, Aase K, Karlsson L, Abramsson A, Uutela M, Backstrom G, Hellstrom M, Bostrom H, Li H, Soriano P, Betsholtz C, et al. PDGF-C is a new protease-activated ligand for the PDGF alpha-receptor. Nat Cell Biol 2000; 2:302–309.

10. Anderberg C, Li H, Fredriksson L, Andrae J, Betsholtz C, Li X, Eriksson U, Pietras K. Paracrine signaling by platelet-derived growth factor-CC promotes tumor growth by recruitment of cancer-associated fibroblasts. Cancer Res 2009; 69:369–378.

11. Crawford Y, Kasman I, Yu L, Zhong C, Wu X, Modrusan Z, Kaminker J, Ferrara N. PDGF-C mediates the angiogenic and tumorigenic properties of fibroblasts associated with tumors refractory to anti-VEGF treatment. Cancer Cell 2009; 15:21–34.

12. Reigstad LJ, Varhaug JE, Lillehaug JR. Structural and functional specificities of PDGF-C and PDGF-D, the novel members of the platelet-derived growth factors family. FEBS J 2005; 272:5723–5741.

13. Shinkai Y, Rathbun G, Lam KP, Oltz EM, Stewart V, Mendelsohn M, Charron J, Datta M, Young F, Stall AM, et al. RAG-2-deficient mice lack mature lymphocytes owing to inability to initiate V(D)J rearrangement. Cell 1992; 68:855–867.

14. Sturn A, Quackenbush J, Trajanoski Z. Genesis: cluster analysis of microarray data. Bioinformatics 2002; 18:207–208.

15. Suo G, Sadarangani A, Lamarca B, Cowan B, Wang JY. Murine xenograft model for human uterine fibroids: an in vivo imaging approach. Reproductive Sciences OnlineFirst [Internet]. 2009. Available from: http://rsx.sagepub.com/cgi/content/abstract/1933719109336615v2.

16. Kuo C, Coquoz O, Troy TL, Xu H, Rice BW. Three-dimensional reconstruction of in vivo bioluminescent sources based on multispectral imaging. J Biomed Opt 2007; 12:024007.

17. Rice BW, Cable MD, Nelson MB. In vivo imaging of light-emitting probes. J Biomed Opt 2001; 6:432–440.

18. Liang M, Wang H, Zhang Y, Lu S, Wang Z. Expression and functional analysis of platelet-derived growth factor in uterine leiomyomata. Cancer Biol Ther 2006; 5:28–33.

19. Kim R, Emi M, Arihiro K, Tanabe K, Uchida Y, Toge T. Chemo-sensitization by STI571 targeting the platelet-derived growth factor/platelet-derived growth factor receptor-signaling pathway in the tumor

20. Li L, Blumenthal DK, Masaki T, Terry CM, Cheung AK. Differential effects of imatinib on PDGF-induced proliferation and PDGF receptor signaling in human arterial and venous smooth muscle cells. J Cell Biochem 2006; 99:1553–1563.

21. Weisberg E, Manley PW, Cowan-Jacob SW, Hochhaus A, Griffin JD. Second generation inhibitors of BCR-ABL for the treatment of imatinib-resistant chronic myeloid leukaemia. Nat Rev Cancer 2007; 7:345–356.

22. Hwu YM, Li SH, Lee RK, Tsai YH, Yeh TS, Lin SY. Increased expression of platelet-derived growth factor C messenger ribonucleic acid in uterine leiomyomata. Fertil Steril 2008; 89:468–471.

23. Zaitseva M, Vollenhoven BJ, Rogers PA. In vitro culture significantly alters gene expression profiles and reduces differences between myome-trial and fibroid smooth muscle cells. Mol Hum Reprod 2006; 12:187–207.

24. Millette E, Rauch BH, Defawe O, Kenagy RD, Daum G, Clowes AW. Platelet-derived growth factor-BB-induced human smooth muscle cell proliferation depends on basic FGF release and FGFR-1 activation. Circ Res 2005; 96:172–179.

25. Fredriksson L, Li H, Fieber C, Li X, Eriksson U. Tissue plasminogen activator is a potent activator of PDGF-CC. EMBO J 2004; 23:3793–3802.

26. Su EJ, Fredriksson L, Geyer M, Folestad E, Cale J, Andrae J, Gao Y, Pietras K, Mann K, Yepes M, Strickland DK, Betsholtz C, et al. Activation of PDGF-CC by tissue plasminogen activator impairs blood-brain barrier integrity during ischemic stroke. Nat Med 2008; 14:731–737.

27. Lei H, Velez G, Hovland P, Hirose T, Kazlauskas A. Plasmin is the major protease responsible for processing PDGF-C in the vitreous of patients with proliferative vitreoretinopathy. Invest Ophthalmol Vis Sci 2008; 49: 42–48.

28. Capdeville R, Buchdunger E, Zimmermann J, Matter A. Glivec (STI571, imatinib), a rationally developed, targeted anticancer drug. Nat Rev Drug Discov 2002; 1:493–502.

29. Rix U, Hantschel O, Durnberger G, Remsing Rix LL, Planyavsky M, Fernbach NV, Kaupe I, Bennett KL, Valent P, Colinge J, Kocher T, Superti-Furga G. Chemical proteomic profiles of the BCR-ABL inhibitors imatinib, nilotinib, and dasatinib reveal novel kinase and nonkinase targets. Blood 2007; 110:4055–4063.

progression and angiogenesis of gastric carcinoma. Cancer 2005; 103: 1800–1809.